

White matter diffusion estimates in obsessive-compulsive disorder across 1653 individuals: machine learning findings from the ENIGMA OCD Working Group

Journal Article

Author(s):

Kim, Bo-Gyeom; Kim, Gakyung; Abe, Yoshinari; Alonso, Pino; Ameis, Stephanie; Anticevic, Alan; Arnold, Paul D.; Balachander, Srinivas; Banaj, Nerisa; Bargalló, Nuria; Batistuzzo, Marcelo C.; Benedetti, Francesco; Bertolín, Sara; Beucke, Jan Carl; Bollettini, Irene; Brem, Silvia; Brennan, Brian P.; Buitelaar, Jan K.; Calvo, Rosa; Castelo-Branco, Miguel; Walitza, Susanne; et al.; ENIGMA-OCD Working Group; Feusner, Jamie D.; Grünblatt, Edna; Kathmann, Norbert; Walitza, Susanne; et al.

Publication date:

2024

Permanent link:

<https://doi.org/10.3929/ethz-b-000668660>

Rights / license:

[Creative Commons Attribution 4.0 International](#)

Originally published in:

Molecular Psychiatry, <https://doi.org/10.1038/s41380-023-02392-6>

ARTICLE OPEN



White matter diffusion estimates in obsessive-compulsive disorder across 1653 individuals: machine learning findings from the ENIGMA OCD Working Group

Bo-Gyeom Kim^{1,148}, Gakyung Kim^{2,148}, Yoshinari Abe³, Pino Alonso^{4,5,6}, Stephanie Ameis^{7,8,9}, Alan Anticevic¹⁰, Paul D. Arnold^{11,12}, Srinivas Balachander¹³, Nerisa Banaj¹⁴, Nuria Bargallo^{15,16}, Marcelo C. Batistuzzo^{17,18}, Francesco Benedetti^{19,20}, Sara Bertolin^{5,21}, Jan Carl Beucke^{22,23,24}, Irene Bollettini²⁰, Silvia Brem^{25,26}, Brian P. Brennan^{27,28}, Jan K. Buitelaar^{29,30}, Rosa Calvo^{5,31,32,33}, Miguel Castelo-Branco^{34,35,36}, Yuqi Cheng³⁷, Ritu Bhusal Chhatkuli^{38,39}, Valentina Ciullo¹⁴, Ana Coelho^{40,41,42}, Beatriz Couto^{40,41,42}, Sara Dallaspesza⁴³, Benjamin A. Ely⁴⁴, Sónia Ferreira^{40,41,42}, Martine Fontaine⁴⁵, Jean-Paul Fouché⁴⁶, Rachael Grazioplene¹⁰, Patricia Gruner¹⁰, Kristen Hagen^{47,48}, Bjarne Hansen^{48,49}, Gregory L. Hanna⁵⁰, Yoshiyuki Hirano^{38,39}, Marcelo Q. Höxter¹⁷, Morgan Hough⁵¹, Hao Hu⁵², Chaim Huyser^{53,54}, Toshikazu Ikuta⁵⁵, Neda Jahanshad⁵⁶, Anthony James⁵⁷, Fern Jaspers-Fayer^{58,59}, Selina Kasprzak^{60,61}, Norbert Kathmann²², Christian Kaufmann²², Minah Kim^{62,63}, Kathrin Koch^{64,65}, Gerd Kvale^{48,66}, Jun Soo Kwon^{63,67,68}, Luisa Lazaro^{5,31,32,33}, Junhee Lee^{62,69}, Christine Lochner⁷⁰, Jin Lu⁷¹, Daniela Rodriguez Manrique^{64,65,72}, Ignacio Martínez-Zalacain^{4,73}, Yoshitada Masuda⁷⁴, Koji Matsumoto⁷⁴, Maria Paula Maziero^{75,76}, Jose M. Menchón^{4,5,6}, Luciano Minuzzi^{77,78}, Pedro Silva Moreira^{40,41,79}, Pedro Morgado^{40,41,42}, Janardhanan C. Narayanaswamy¹³, Jin Narumoto⁸⁰, Ana E. Ortiz^{31,32,33}, Junko Ota^{38,39}, Jose C. Pariente¹⁶, Chris Perriello⁸¹, Maria Picó-Pérez^{40,41,82}, Christopher Pittenger^{10,83,84,85}, Sara Poletti²⁰, Eva Real^{5,6}, Y. C. Janardhan Reddy¹³, Daan van Rooij⁸⁶, Yuki Sakai^{80,87}, João Ricardo Sato^{88,89}, Cinto Segalas^{5,6}, Roseli G. Shavitt⁹⁰, Zonglin Shen³⁷, Eiji Shimizu^{38,39,91}, Venkataram Shivakumar⁹², Noam Soreni^{93,94}, Carles Soriano-Mas^{5,6,95}, Nuno Sousa^{40,41,42}, Mafalda Machado Sousa^{40,41,42}, Gianfranco Spalletta^{14,96}, Emily R. Stern^{97,98}, S. Evelyn Stewart^{58,99,100}, Philip R. Szeszko^{101,102}, Rajat Thomas¹⁰³, Sophia I. Thomopoulos⁵⁶, Daniela Vecchio¹⁴, Ganesan Venkatasubramanian¹³, Chris Vriend^{60,61,104}, Susanne Walitza^{25,26}, Zhen Wang¹⁰⁵, Anri Watanabe⁸⁰, Lidewij Wolters¹⁰⁶, Jian Xu¹⁰⁷, Kei Yamada¹⁰⁸, Je-Yeon Yun^{109,110}, Mojtaba Zarei¹¹¹, Qing Zhao¹⁰⁵, Xi Zhu^{112,113} and, ENIGMA-OCD Working Group*, Paul M. Thompson⁵⁶, Willem B. Bruin^{104,114}, Guido A. van Wingen^{104,114}, Federica Piras¹⁴, Fabrizio Piras¹⁴, Dan J. Stein^{115,116}, Odile A. van den Heuvel^{60,61}, Helen Blair Simpson⁴⁵, Rachel Marsh⁴⁵ and Jiook Cha^{1,2,23}

© The Author(s) 2024, corrected publication 2024

White matter pathways, typically studied with diffusion tensor imaging (DTI), have been implicated in the neurobiology of obsessive-compulsive disorder (OCD). However, due to limited sample sizes and the predominance of single-site studies, the generalizability of OCD classification based on diffusion white matter estimates remains unclear. Here, we tested classification accuracy using the largest OCD DTI dataset to date, involving 1336 adult participants (690 OCD patients and 646 healthy controls) and 317 pediatric participants (175 OCD patients and 142 healthy controls) from 18 international sites within the ENIGMA OCD Working Group. We used an automatic machine learning pipeline (with feature engineering and selection, and model optimization) and examined the cross-site generalizability of the OCD classification models using leave-one-site-out cross-validation. Our models showed low-to-moderate accuracy in classifying (1) “OCD vs. healthy controls” (Adults, receiver operator characteristic-area under the curve = 57.19 ± 3.47 in the replication set; Children, 59.8 ± 7.39), (2) “unmedicated OCD vs. healthy controls” (Adults, 62.67 ± 3.84 ; Children, 48.51 ± 10.14), and (3) “medicated OCD vs. unmedicated OCD” (Adults, 76.72 ± 3.97 ; Children, 72.45 ± 8.87). There was significant site variability in model performance (cross-validated ROC AUC ranges 51.6–79.1 in adults; 35.9–63.2 in children). Machine learning interpretation showed that diffusivity measures of the corpus callosum, internal capsule, and posterior thalamic radiation contributed to the classification of OCD from HC. The classification performance appeared greater than the model trained on grey matter morphometry in the prior ENIGMA OCD study (our study includes subsamples from the morphometry study). Taken together, this study points to the meaningful multivariate patterns of white matter features relevant to the neurobiology of OCD, but with low-to-moderate classification accuracy. The OCD classification performance may be constrained by site variability and medication effects on the white matter integrity, indicating room for improvement for future research.

Molecular Psychiatry; <https://doi.org/10.1038/s41380-023-02392-6>

A full list of author affiliations appears at the end of the paper.

Received: 29 March 2023 Revised: 27 November 2023 Accepted: 19 December 2023

Published online: 07 February 2024

INTRODUCTION

Obsessive-compulsive disorder (OCD) is a common, often chronic psychiatric disorder, affecting 1.0–1.5% of the global population over their lifetime [1]. Extensive neuroimaging research suggests structural and functional abnormalities in cortico-striato-thalamo-cortical (CSTC) circuits in OCD [2–7]. The field has also started to address the question of whether multivariate analyses of neuroimaging data can be used to classify OCD [8, 9].

Prior OCD studies with relatively small to modest samples show mixed findings, with OCD classification accuracies varying from 66% to 100% [8]. However, the generalizability of such findings has rarely been tested, and reproducibility failures have been a major challenge in psychiatric neuroimaging [9–12]. Indeed, typical single-site neuroimaging studies seeking brain-wide associations with psychopathology using small sample sizes of tens to hundreds of individuals may report inflated effect sizes, decreasing reproducibility [13].

The ENIGMA-OCD consortium has allowed rigorous mega-analyses and meta-analyses based on the largest international multisite neuroimaging datasets to date [9]. A machine learning analysis of regional measures of cortical thickness, surface area and subcortical volume found that model performance did not exceed chance-level, but that classification performance was improved when individuals with OCD were grouped according to medication status.

Altered white matter pathways have been implicated in the neurobiology of OCD [14]. An ENIGMA-OCD study using diffusion tensor imaging reported significantly lower fractional anisotropy (FA) in the sagittal striatum (SS) and posterior thalamic radiation (PTR), higher mean diffusivity (MD) in the SS and higher radial diffusivity (RD) in SS and PTR [15]. However, the question of whether white matter diffusion tensor imaging findings can be

used to classify OCD has not yet been explored in large and multisite studies.

In this study, we therefore used ENIGMA-OCD on diffusion tensor imaging to test the classification power of such measures in a large multisite sample of individuals with OCD and healthy controls. We tested several machine learning algorithms to distinguish those with OCD versus healthy controls, as well as to distinguish OCD individuals off medication versus healthy controls, and to distinguish OCD individuals on versus off medication. We also assessed the site-variability and reproducibility of predictive models using leave-one-site-out cross-validation and evaluated the utility of a post-processing harmonization tool (i.e., NeuroComBat). Finally, we employed a machine learning interpretation framework to assess which features were most relevant to the various classifications.

PARTICIPANTS AND METHODS

Participants

Data from the ENIGMA-OCD Working Group recruited from 18 international research institutes were used. We analyzed data from 1653 participants, including 1336 adult participants (429 unmedicated OCD, 261 medicated OCD, 646 HC) and 317 pediatric participants (70 unmedicated OCD, 105 medicated OCD, 142 HC) (Table 1). Here, we defined pediatrics as under the age of 18 years old, consistent with previous work from the ENIGMA-OCD working group [2, 9]. The diagnosis of OCD and other comorbid conditions (i.e., anxiety disorders and major depressive disorder) were assessed using DSM-IV criteria (American Psychiatric Association, 2000). Clinical characteristics included medication status, childhood-onset, disease duration (in years), symptom severity (total scores ranging from 0–40 on the (Child) Yale-Brown Obsessive-Compulsive Scale ((C)Y-BOCS) [16, 17] and current or lifetime history of symptom dimensions (i.e., aggression/checking, cleaning/contamination, sexual/religious, hoarding, ordering/symmetry). Participants who did not

Table 1. Demographic and clinical characteristics of patients with obsessive-compulsive disorder (OCD) and healthy controls (HCs).

Characteristics	Adult OCD sample (<i>n</i> = 690)	Adult HC sample (<i>n</i> = 646)	Pediatric OCD sample (<i>n</i> = 175)	Pediatric HC sample (<i>n</i> = 142)
Demographic Characteristics				
Age (years)	31.6 ± 9.78	30.8 ± 9.97	14.5 ± 2.3	14.3 ± 2.4
Male <i>N</i> (%)	397 (25.6)	380 (24.2)	97 (27.8)	77 (22.1)
Clinical Characteristics				
OCD illness severity score	25 ± 7.11		20.8 ± 8.0	
Childhood-onset <i>N</i> (%)	351 (51.7)			
Duration of illness	12.4 ± 11.1		3.0 ± 2.5	
Medication use at time of scan <i>N</i> (%)	261 (37.8)		105 (60)	
Lifetime diagnosis				
Anxiety	76 (11.02)		48 (27.4)	
Major depression	84 (12.17)		18 (10.3)	
Current comorbid disorders				
Anxiety	69 (10.0)		29 (16.6)	
Major depression	77 (11.2)		6 (3.4)	
OCD symptom dimension				
Aggressive/checking	411 (59.6)		73 (41.7)	
Contamination/cleaning	355 (51.5)		62 (35.4)	
Symmetry/ordering	370 (53.6)		68 (38.9)	
Sexual/religious	228 (33.0)		55 (31.43)	
Hoarding	114 (16.5)		47 (26.9)	

Symptom score was indicated by total score on the adult and child version of the Yale-Brown Obsessive Compulsive Scales. OCD symptom dimensions were measured with the YBOCS symptom checklist.

have medication information were excluded from the medication classification analysis.

Image acquisition and processing

Image preprocessing, including brain extraction, eddy current correction, movement correction, echo-planar imaging-induced distortion correction, and tensor fitting, was conducted at each site, and Tract-Based Spatial Statistics (TBSS) was performed using protocols and quality control pipelines provided by the ENIGMA-DTI working group (<http://enigma.ini.usc.edu/protocols/dti-protocols/>) [15]. For the entire skeleton in each hemisphere, four DTI measures (FA, MD, AD, and RD) were estimated within 25 tract-wise regions of interest (ROIs) based on the Johns Hopkins University (JHU) white matter parcellation atlas [15].

OCD classification with machine learning

We conducted automated machine learning (AutoML) with H2O Driverless Artificial Intelligence (AI) (DAI, 1.8.7.1 version) using white matter anisotropy and diffusivity estimates (FA, MD, AD, RD; $N = 252$; $4 * \{(19 \text{ fascicles} * 3 \text{ (left, right, total)} + 5 \text{ fascicles (total; e.g., corpus callosum, fornix)} + \text{average metrics across all fascicles})\}$ and biological variables (age, sex). Three classification models were built in adult and pediatric samples, separately: (1) OCD vs. HC, (2) unmedicated OCD vs. HC (to test the effects of pure OCD—not confounded by medication effects—on the white matter), (3) medicated OCD vs. unmedicated OCD (to test the medication effects on the white matter). To prevent data leakage and reduce model overfitting, we split the entire data into a discovery set (80%) and a replication set (20%) (stratified by diagnosis). In the discovery set, we used leave-one-site-out (LOSO) cross-validation (11 sites for adults, seven sites for pediatrics) (Supplementary Fig. 1). With this scheme, within the discovery set, we evaluated the cross-site variability (or generalizability); within the replication set, we tested the overall model generalizability considering potential site variability. The test samples of the discovery data were not used during model optimization. The machine learning pipeline in AutoML involves the estimation of several base models (e.g., XGBoost, LightGBM, the general linear model (GLM)) and stacked ensemble models [18] derived from base models. The AutoML pipeline performs random hyperparameter tuning along with feature transformation (e.g., interaction encoding, numeric to categorical target encoding). Firstly, in each iteration, models learn and update the weights of the features and select important features based on the prior iteration. Then, the pipeline searches for the best feature transformations and model parameters using genetic algorithm [19]. In DAI, this procedure is called “feature evolution”. In genetic algorithm’s evolution can be seen as a competition between mutating parameters to find best “individuals” referring to information about feature transformations and hyperparameters. The feature evolution procedure is not entirely random and is informed from the variable importance interactions obtained from the modeling algorithms. So, this model training procedure including feature selection, transformation, and hyper-parameter tuning was performed using 11-fold-cross-validation scheme. In each fold, 10 folds were used for training the model, while the remaining 1-fold was used to (cross)validate the best training model. Finally, the best cross-validation models from each fold were combined and tested on a held-out replication set. In this way, the validation data within the 11-fold cross validation was not used for model optimization and feature evolution. Likely, replication data was not used for data preprocessing, model training or optimization. We used the ROC-AUC as the primary performance metric and accuracy, sensitivity, and specificity as additional metrics. pROC v. 1.16.2 in the R programming language was used to calculate the metrics [20].

NeuroComBat harmonization

To reduce potential biases caused by site and scanner effects, we employed NeuroComBat harmonization [21]. ComBat, a short name for combatting batch effects when combining multiple batches [21, 22], corrects potential scanner/site effects on brain data by harmonizing the mean and variance of brain measures across scanners. We harmonized the diffusivity measures in the discovery and replication data separately while also including age and sex as covariates in the model matrix. Non-parametric empirical Bayes adjustments were used to adjust for batch effects.

Model interpretation

To interpret the machine learning classifiers, we calculated the relative weights of DTI features contributing to OCD classification. We used two

steps to determine the relative weights of DTI features contributing to OCD classification. First, we calculated the relative weights of each base model according to the model-specific algorithm. For LightGBM and XGBoostGBM, DAI computed the average reduction in impurity across all trees. Second, the importance of each base model was multiplied by its weight and normalized. We further implemented a machine learning interpretation framework, K-Local Interpretable Model-agnostic Explanation (K-LIME) [23]. This method fits surrogate linear models to data to extract the important features either positively or negatively associated with a target outcome: (1) OCD vs. HC, (2) unmedicated OCD vs. HC, and (3) medicated OCD vs. unmedicated OCD.

Statistical analysis

To assess the effects of sites on diffusion white matter estimates, we performed principal component analysis (PCA). We tested the association between predicted OCD probabilities and clinical variables (e.g., medication status, childhood-onset) using stepwise regression models [24]. Additionally, we tested site effects on individual classification performances (i.e., whether participants were correctly classified as OCD or HC). To adjust for potential confounding factors, we included the following variables as covariates: age, sex, site, and average DTI metrics (i.e., mean FA, AD, RD, MD).

RESULTS

Demographic characteristics

This study included 1336 adult participants (690 OCD, 646 HC) and 317 pediatric participants (175 OCD, 142 HC). Out of the adult OCD samples, 37.8% were taking medication, while 60% of the pediatric OCD sample were taking medication. OCD patients showed comorbidity with lifetime anxiety disorders (adult: 11.02%, pediatric: 27.4%) and major depressive disorder (adult: 12.2%, pediatric: 10.3%). Table 1 and Supplementary Table 1 contain detailed demographic and clinical characteristics of the participants. Demographic characteristics were not significantly different between OCD and HC (P 's > 0.45). However, the clinical characteristics varied across sites, including childhood-onset: $\chi^2 = 93.66$, $p < 0.001$, and symptom dimensions: Aggression/checking: $\chi^2 = 64.33$, $p < 0.001$, contamination/cleaning: $\chi^2 = 53.02$, $p = 0.002$, sexual/religious: $\chi^2 = 46.33$, $p = 0.012$, hoarding: $\chi^2 = 73.06$, $p < 0.001$, symmetry/ordering: $\chi^2 = 145.03$, $p < 0.001$ in adults. Illness duration also varied across sites in the pediatric samples, $F = 13.20$, $p < 0.001$.

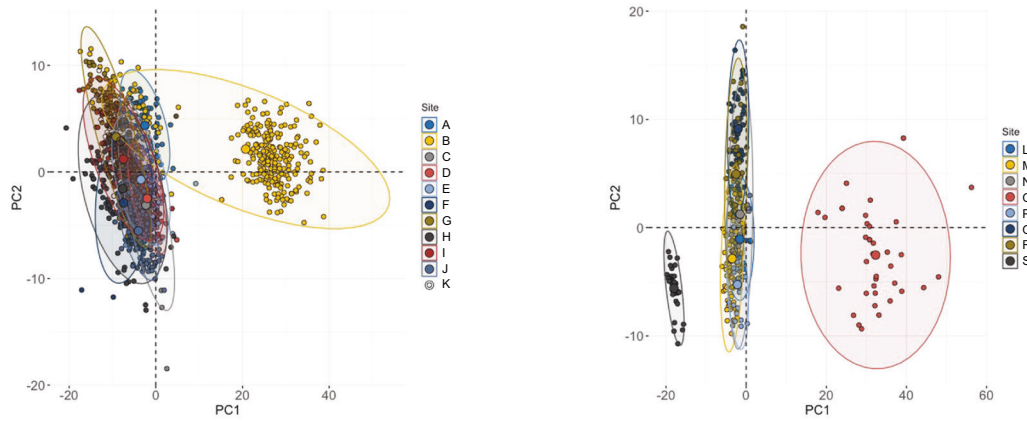
Classification of OCD

The principal component analysis (PCA) of the four-diffusion metrics (FA, MD, AD, RD) across the 18 international sites revealed site variability (Fig. 1). In the PCA biplot, we observed two sites, one from adults and one from pediatrics, which were distinct from other sites. We then performed three classification tasks using the stacked ensemble machine learning models (LOSO cross-validation): (1) OCD vs. HC, (2) unmedicated OCD vs. HC, and (3) unmedicated OCD vs. medicated OCD (Tables 2 and 3, Fig. 2).

In adult samples, the models minimally-to-modestly classified participants with OCD diagnosis from healthy controls in the discovery set ($N = 1068$, ROC AUC = 67.29 ± 0.26) and the replication set ($N = 268$, ROC AUC = 57.19 ± 3.47). The models also minimally-to-modestly distinguished unmedicated OCD versus healthy individuals in the discovery set ($N = 854$, ROC AUC = 63.96 ± 0.43) and the replication set ($N = 214$, ROC AUC = 62.67 ± 3.84). Finally, the models distinguished medicated OCD versus unmedicated OCD participants in the discovery set ($N = 437$, ROC AUC = 60.22 ± 0.40) and the replication set ($N = 137$, ROC AUC = 76.72 ± 3.97).

In pediatric samples, the models classified participants with OCD diagnosis versus healthy controls in the discovery set ($N = 270$, ROC AUC = 69.54 ± 8.59) and the replication set ($N = 64$, ROC AUC = 59.80 ± 7.39). The models also classified unmedicated OCD versus healthy individuals in the discovery set

A. Before applying NeuroCombat harmonization.



B. After applying NeuroCombat harmonization.

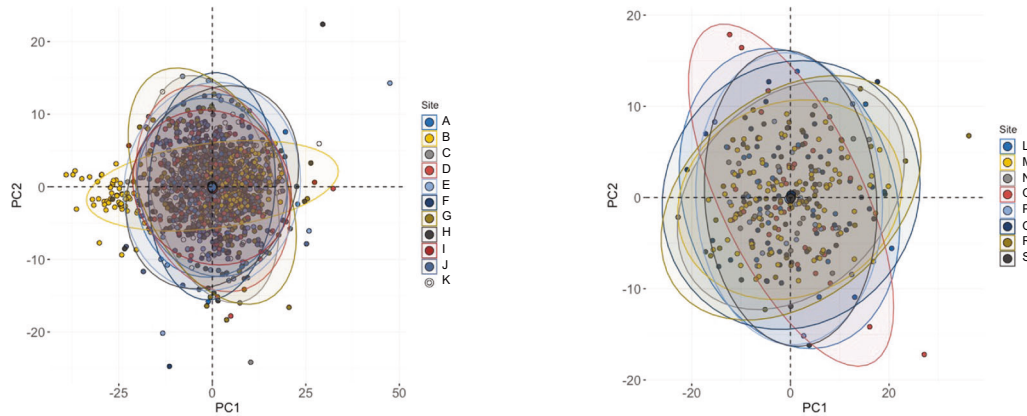


Fig. 1 A biplot of principal component analysis (PCA) using the diffusion tensor estimates of the major white matter fascicles across the 18 international sites. **A** PCA biplot before applying NeuroCombat. (Left: Adult, Right: Pediatric). Some sites (e.g., site B) show apparent clusters distinct from the rest of the sites. **B** PCA biplot after applying NeuroCombat. (Left: Adult, Right: Pediatric).

($N = 151$, ROC AUC = 65.96 ± 12.33) and the replication set ($N = 38$, ROC AUC = 48.51 ± 10.14). Finally, the models classified medicated OCD versus unmedicated OCD participants in the discovery set ($N = 140$, ROC AUC = 61.82 ± 15.50) and the replication set ($N = 35$, ROC AUC = 72.45 ± 8.87) (Table 2C).

In classifying OCD and HC, the ROC AUC of adult samples ranged from 51.6% (site C) to 79.1% (site F), and pediatric samples ranged from 35.9% (site M) to 63.2% (site L) across sites. Also, mean values of DTI metrics across all ROIs showed significant differences across sites ($F_s > 97.4$, $p < 0.001$). The site variability was significantly associated with the classification performance in OCD patients ($\chi^2 = 57.19$, $p < 0.001$) and HCs ($\chi^2 = 50.30$, $p < 0.001$) when adjusting for the covariates (Fig. 3).

Classification of OCD with NeuroCombat-harmonized data

Considering the site variability (Fig. 1), we implemented the ML analysis with NeuroCombat-harmonized data to correct site effects. The NeuroComBat-harmonized data showed slightly lower performance in the adult samples (Table 2A) and slightly higher performance in the pediatric samples (Table 2B).

Variables associated with OCD classification

Results of stepwise regression analysis indicated that, in adults, site (e.g., site H, site I), higher age, hoarding symptoms, and adult-onset were significantly associated with estimated OCD

probabilities ($t > 2.04$, $p < 0.05$) (Table 3). In pediatric samples, site (e.g., site M, site S), lifetime diagnosis of depression, and aggression/checking symptoms significantly correlated with predicted OCD probabilities ($t > 2.15$, $p < 0.05$).

Machine learning interpretation

Our machine learning interpretation models showed that various specific diffusion white matter features contributed to the OCD classification (Figs. 4 and 5, Supplementary Fig. 2). For the classification of OCD from HC in adult samples, the top 10 features included the superior *corona radiata* (MD), age, posterior thalamic radiation (FA), and posterior limb of the internal capsule (FA, AD). In the pediatric samples, the cingulum (MD, AD), uncinate fasciculus (MD), fornix (FA), corticospinal tract (FA), and anterior *corona radiata* (AD) were important in classifying OCD diagnosis (Supplementary Fig. 2). In classifying unmedicated OCD and HC, the internal capsule contributed to both adult (FA, AD of posterior limb) and pediatric samples (FA of the retrolenticular part, AD of anterior limb, FA of posterior limb) (Fig. 4). In classifying medicated OCD and unmedicated OCD in adult samples, the top 10 features included the corpus callosum (total, genu), average FA, and average RD (Supplementary Fig. 2). For the pediatric samples, fornix and stria terminalis, cingulum (cingulate gyrus, hippocampus) were included in the top 10 features (Supplementary Fig. 2).

Table 2. Performance of classification of OCD clinical outcomes in (A) adult, (B) adult applied NeuroComBat harmonization, (C) pediatric, (D) pediatric applied NeuroComBat harmonization samples. — mean with 95% confidence interval.

(A) Adult sample						
	OCD (<i>N</i> = 690) vs. HC (<i>N</i> = 646)		Unmedicated OCD (<i>N</i> = 429) vs. HC (<i>N</i> = 646)		Unmedicated OCD (<i>N</i> = 429) vs. medicated OCD (<i>N</i> = 261)	
	Discovery set	Replication set	Discovery set	Replication set	Discovery set	Replication set
ROC-AUC	67.29 ± 0.26	57.19 ± 3.47	63.96 ± 0.43	62.67 ± 3.84	60.22 ± 0.40	76.72 ± 3.97
Accuracy (%)	66.37 ± 0.27	57.08 ± 3.22	64.64 ± 0.49	61.68 ± 3.58	66.88 ± 0.32	67.15 ± 12.83
Sensitivity (%)	61.96 ± 0.79	75.36 ± 8.49	65.84 ± 1.66	58.82 ± 19.79	58.7 ± 1.53	92.31 ± 2.95
Specificity (%)	71.87 ± 0.73	37.69 ± 29.44	68.44 ± 1.00	63.57 ± 7.92	73.77 ± 1.44	51.76 ± 16.19
(B) Adult sample, NeuroComBat						
	OCD (<i>N</i> = 690) vs. HC (<i>N</i> = 646)		Unmedicated OCD (<i>N</i> = 429) vs. HC (<i>N</i> = 646)		Unmedicated OCD (<i>N</i> = 429) vs. medicated OCD (<i>N</i> = 261)	
	Discovery set	Replication set	Discovery set	Replication set	Discovery set	Replication set
ROC-AUC	64 ± 0.05	51.07 ± 3.54	67.35 ± 0.52	52.8 ± 4.18	66.12 ± 3.63	62.24 ± 5.08
Accuracy (%)	63.87 ± 0.07	53.36 ± 3.64	66.44 ± 0.52	60.75 ± 3.09	74.42 ± 0.65	68.6 ± 3.72
Sensitivity (%)	67.14 ± 1.20	37.68 ± 25.16	63.95 ± 1.80	37.65 ± 17.42	76.14 ± 0.71	48.08 ± 13.79
Specificity (%)	60.96 ± 1.24	70 ± 13.74	71.55 ± 0.87	75.97 ± 9.51	70.31 ± 1.35	81.18 ± 4.19
(C) Pediatric sample						
	OCD (<i>N</i> = 175) vs. HC (<i>N</i> = 142)		Unmedicated OCD (<i>N</i> = 105) vs. HC (<i>N</i> = 142)		Unmedicated OCD (<i>N</i> = 105) vs. medicated OCD (<i>N</i> = 70)	
	Discovery set	Replication set	Discovery set	Replication set	Discovery set	Replication set
ROC-AUC	69.54 ± 8.59	59.8 ± 7.39	65.96 ± 12.33	48.51 ± 10.14	61.82 ± 15.50	72.45 ± 8.87
Accuracy (%)	73.56 ± 6.82	62.5 ± 6.38	69.15 ± 8.35	57.9 ± 8.06	69.15 ± 11.18	74.3 ± 5.83
Sensitivity (%)	73.25 ± 17.25	65.71 ± 16.03	73.43 ± 14.12	50 ± 25.51	73.43 ± 12.74	95.24 ± 2.43
Specificity (%)	73.03 ± 13.18	58.62 ± 20.58	68.75 ± 9.90	62.5 ± 19.13	68.75 ± 15.95	42.86 ± 29.15
(D) Pediatric sample, NeuroComBat						
	OCD (<i>N</i> = 175) vs. HC (<i>N</i> = 142)		Unmedicated OCD (<i>N</i> = 105) vs. HC (<i>N</i> = 142)		Unmedicated OCD (<i>N</i> = 105) vs. medicated OCD (<i>N</i> = 70)	
	Discovery set	Replication set	Discovery set	Replication set	Discovery set	Replication set
ROC-AUC	66.05 ± 0.41	60.49 ± 7.20	60.71 ± 0.92	55.36 ± 10.15	66.78 ± 0.35	58.2 ± 8.85
Accuracy (%)	67.56 ± 0.38	62.5 ± 6.38	61.46 ± 0.28	71.05 ± 8.06	72.1 ± 0.28	60 ± 5.82
Sensitivity (%)	62.28 ± 1.55	71.43 ± 13.10	84.06 ± 0.91	35.71 ± 25.51	77.5 ± 0.91	47.61 ± 2.43
Specificity (%)	77.16 ± 1.46	51.72 ± 24.63	54.69 ± 2.05	91.67 ± 19.13	68.75 ± 2.05	78.57 ± 29.15

For the classification of medication status among OCD patients, some sites (i.e., Amsterdam, Shanghai) containing only unmedicated OCD were excluded from the discovery set.

For the classification of medication status among OCD patients, some sites (i.e., Calgary) containing only unmedicated OCD were excluded from the discovery set.

DISCUSSION

In this study, we tested the extent to the accuracy of machine learning in classifying the diagnosis or medication status of OCD patients based on white matter diffusion estimates obtained using the ENIGMA-matched image analysis pipeline across 18 international sites. Our results showed a low-to-moderate accuracy in predicting OCD diagnosis and medication status. Classification of medicated OCD versus unmedicated OCD had the best classification accuracy (ROC-AUC of 76.72 in adults), followed by unmedicated OCD-health control classification (ROC-AUC of 63.96 in adults) and all OCD-HC (ROC-AUC of 57.19 in adults). In all OCD-HC classifications, the performance varied significantly across sites with cross-validated ROC AUC ranging 51.6–79.1 in adults, and 35.9–63.2 in children. Diffusion white matter features contributing to OCD classification (compared with HC) include anisotropy and diffusivity estimates of white matter in the internal capsule, thalamic radiation, and uncinate fasciculus.

The low-to-moderate accuracy of our machine learning models is consistent with prior work. OCD machine learning studies using structural MRI have found that accuracy in classifying OCD and HC, ranges from 60 to 90%, all in small datasets (*N* < 150) [8, 10]. However, these classification performances from small studies are likely to be inflated and not generalizable, while the true effect size (i.e., the brain-psychopathology association, regardless of the choice of analysis) may be smaller [13]. Indeed, a recent large-scale ENIGMA OCD study found that machine learning models trained on gray matter morphometric estimates from structural MRI resulted in poor classification of OCD vs. HC (ROC AUC, 51–54; leave-one-site CV) [9]. Our model based on white matter features showed improved classification performance compared with the gray matter morphometry model in adults and pediatric samples, though a direct comparison may not be warranted due to different machine learning pipelines and different subsamples used in this study. Future studies should determine whether multi-

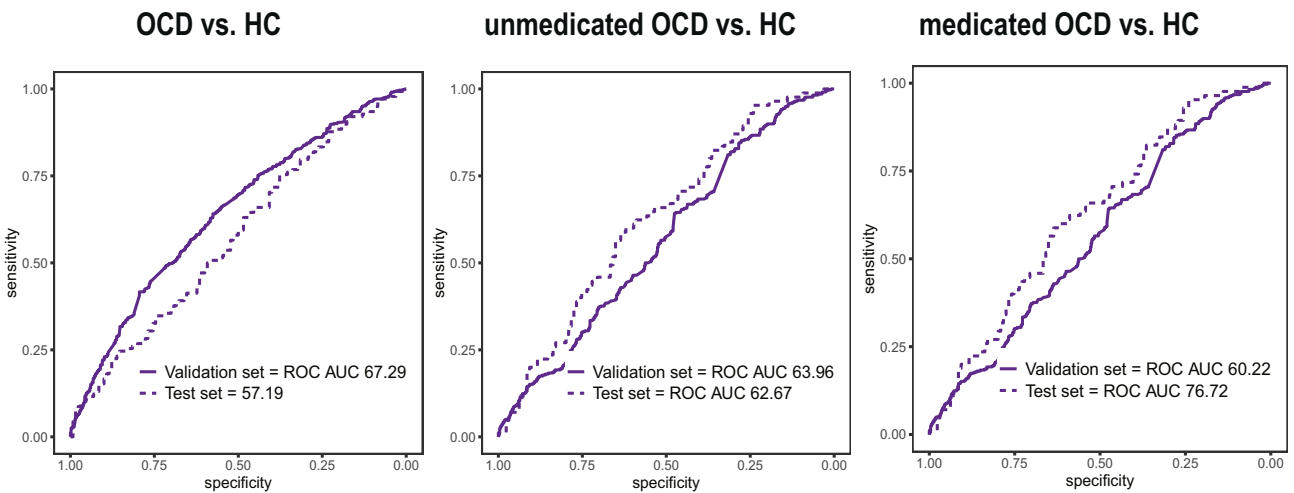
Table 3. The association between brain-predicted OCD risk probabilities and clinical features in a discovery set (stepwise regression).

Variable	Beta	F	P value	η^2
(A) Adult sample, Discovery set (OCD = 379) (Adjusted = 15.15%)				
Site		6.996	7.72E-08	0.118
Age	0.011	16.152	7.10E-05	0.042
Hoarding	0.017	8.316	0.004	0.022
Childhood-onset	-0.010	4.172	0.042	0.011
Current Depression	0.015	2.372	0.124	0.006
(B) Pediatric sample, Discovery set (OCD = 55) (Adjusted = 32.89%)				
Site		11.796	6.57E-05	0.325
Depression	-0.13142	5.062	0.029	0.094
Aggression, Checking	-0.0645	4.619	0.037	0.086
Age	0.02355	1.896	0.175	0.037

modal machine learning using structural and functional MRI can increase classification accuracy [25–28].

We observed significant site variability in classification performance. Firstly, this may be related to the variability of the quality of the diffusion MRI across sites. The aggregated ENIGMA MRI data were harmonized for the post-imaging processing procedure (e.g., TBSS) but not for data acquisition. Though this harmonization method was a best practice when the raw image data were not sharable, nevertheless, given the sensitivity of diffusion MRI to the image acquisition conditions (e.g., magnets types, pulse sequences, such as numbers of gradient directions or b values, etc.; compared with the gray matter morphometry validated across scanners, sites, and pulse sequence designs [29]), our approach is limited in controlling potential confounding factors and their impact on the quality of the diffusion white matter metrics. Also, our application of another post-processing harmonization method, NeuroComBat, was effective in matching the distributions of the data across the sites (in our PCA results). However, this method failed to result in a performance gain in the OCD classification (slightly higher AUC in pediatric samples, slightly lower AUC in adult samples) or a reduction of the cross-

A. Adult



B. Pediatric

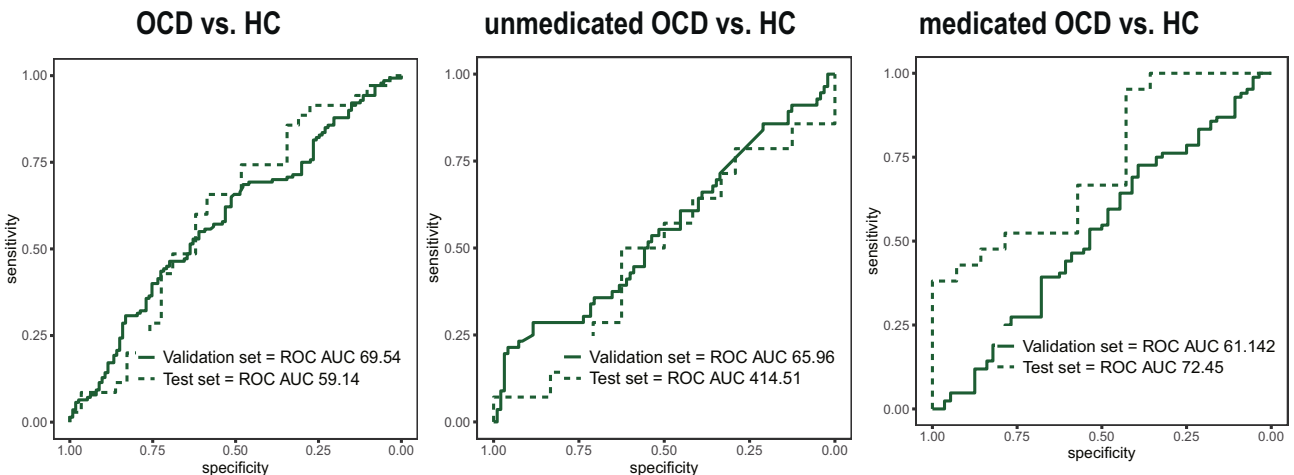
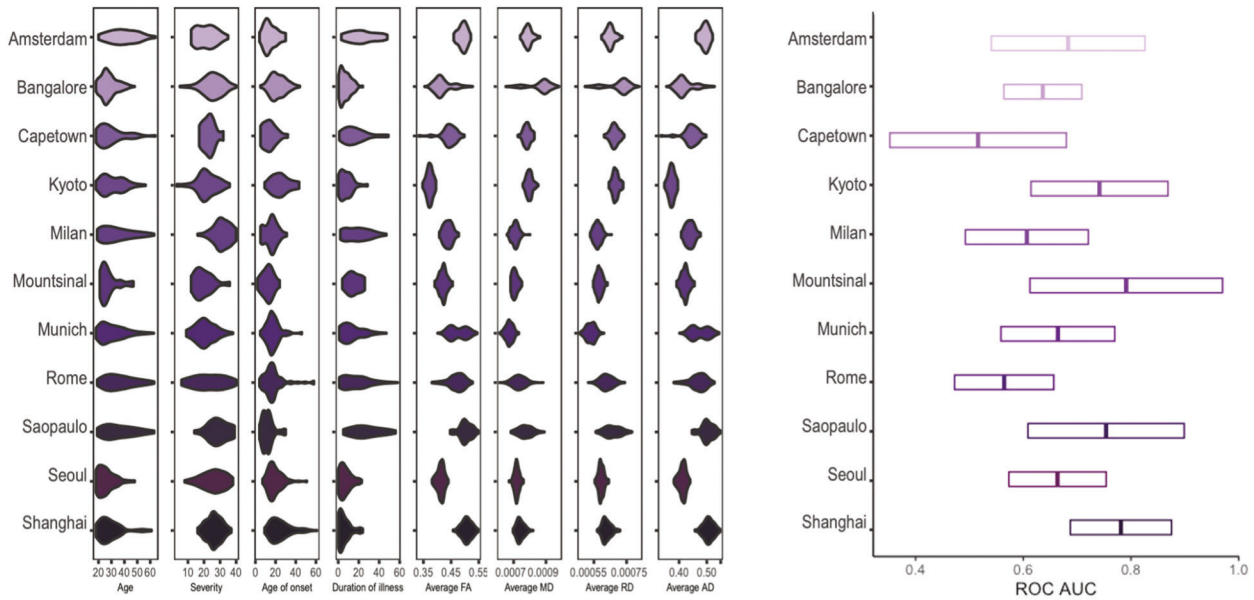


Fig. 2 Classification of OCD diagnosis and medication status using diffusion tensor estimates. **A** Classification performances in adult samples. **B** Classification performances in pediatric samples.

A. Adult



B. Pediatric

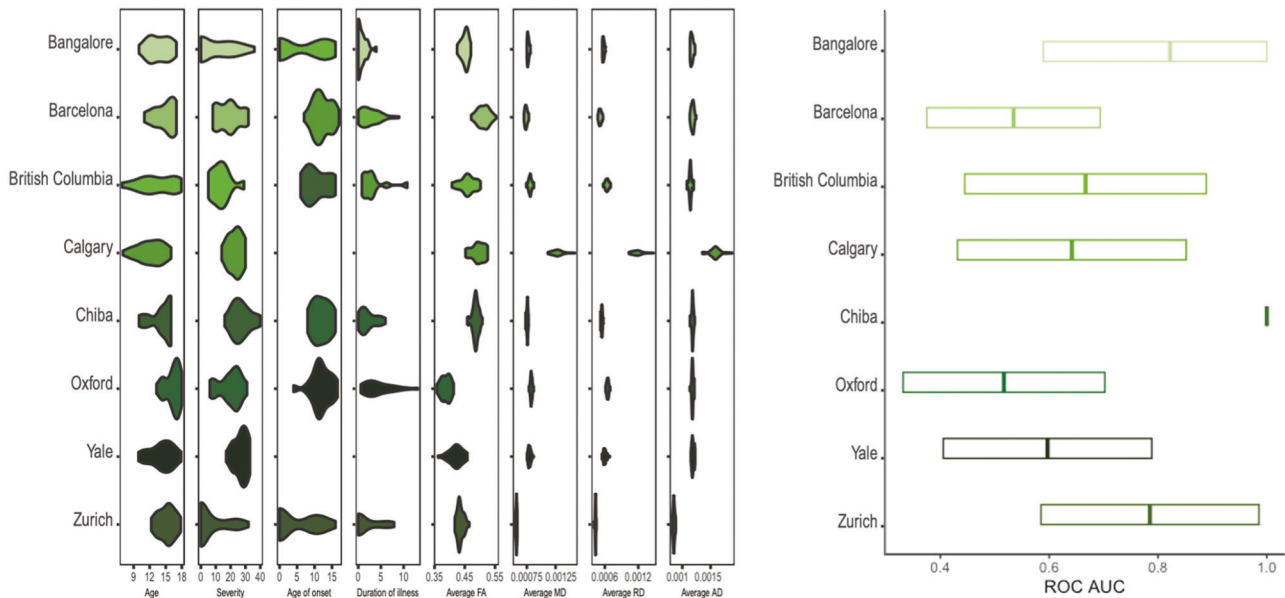


Fig. 3 Sample characteristics and prediction performance (ROC AUC) across sites. A In adult samples. **B** In pediatric samples. Left: Violin plots of sociodemographic, clinical, and 763 brain features across sites, Right: Box plot of the area under the receiver operating 764 characteristic curve (ROC AUC) for the leave-one-site-out (LOSO) cross validation in the 765 diagnosis classification task (OCD vs. HC).

site variability. The covariate modeling with NeuroComBat also did not demonstrate a gain in performance. Secondly, our international multisite clinical samples show variability in clinical characteristics such as symptom severity, age, adult-onset, and duration of illness. The sampling variability may have added complexity to the already challenging task of OCD classification.

Our analysis of the machine learning model indicated that OCD probability was significantly associated with several sociodemographic and clinical characteristics. In adults with OCD, a higher age, adult onset, greater hoarding symptoms, and greater depressive symptoms were more likely to be predicted as having OCD. The significant correlation of age and adult-onset with the OCD likelihood might reflect age-dependent patterns in the diffusion white matter estimates. Though there are no significant group differences in age

between OCD and HC, the neurobiology of OCD might be related to abnormal aging effects on the diffusion white matter estimates. Indeed, some literature shows that psychiatric disorders, including OCD and anxiety disorders, are linked to accelerated brain aging [30, 31]. However, the potential association between the neuropathophysiology of OCD and age appears more relevant to adults than to children because, despite the similar effect sizes of age and the OCD likelihood, only adult samples show statistical significance (probably due to a larger sample size). This may reflect the effects of chronicity in adult samples [32].

Our machine learning interpretation is consistent with prior white matter studies that have relied on univariate analyses and/or small sample sizes [33]. For example, the well-known CTSC pathway includes the internal capsule (posterior limb (FA, AD) in

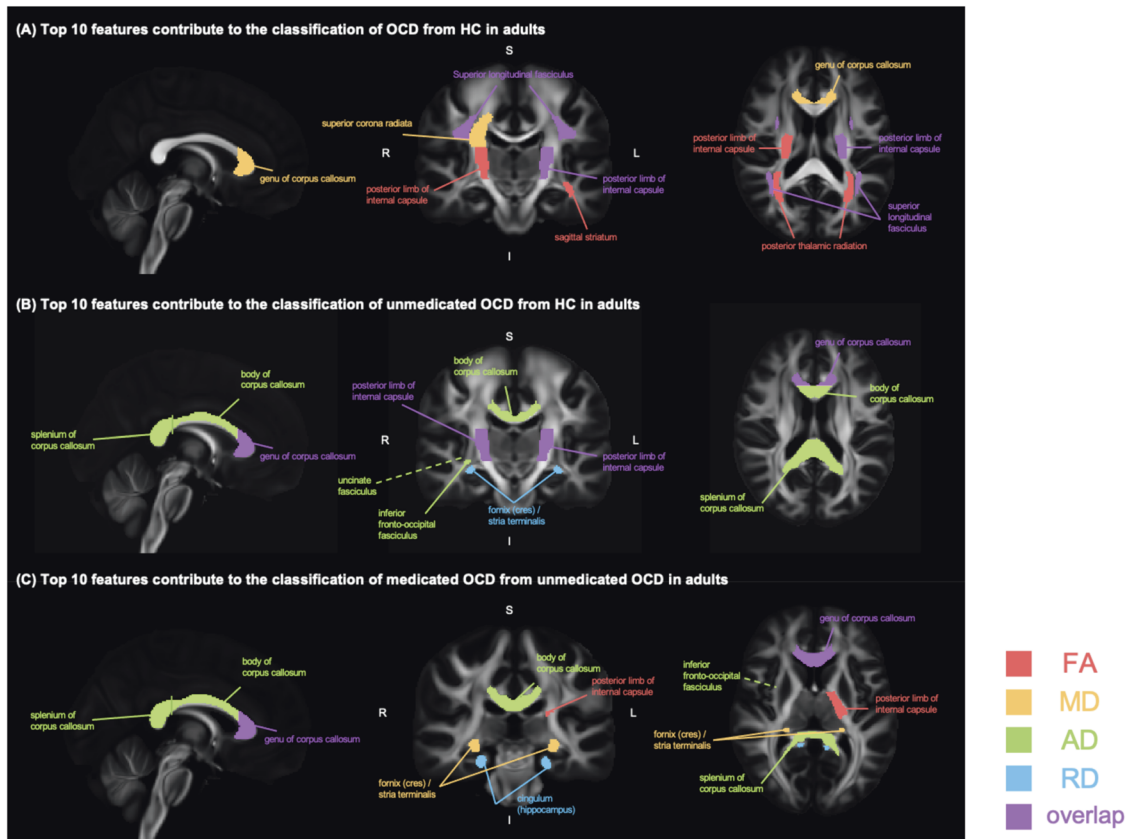


Fig. 4 Top 10 features of classification models in adults. A Top 10 features contribute to the classification of OCD from HC in adults. **B** Top 10 features contribute to the classification of unmedicated OCD from HC in adults. **C** Top 10 features contribute to the classification of medicated OCD from unmedicated OCD in adults. Note: The color legend represents DTI measures: red for FA, yellow for MD, green for AD, and blue for RD. Regions with multiple DTI measures are highlighted in purple.

adults and retrolenticular part (MD) in children), which has been implicated in habit formation and cognitive control in OCD [34]. In the classification model of unmedicated OCD and HC, the corpus callosum - connecting the two cerebral hemispheres - was important in adults and pediatric samples alike. This finding is in line with the previous ENIGMA-OCD study [15] indicating that adult OCD was characterized by lower volume in the genu of the corpus callosum than HC. However, careful interpretation is needed because of differences in the brain metrics used, here based on tensor modeling (FA, MD). In addition, we found that the cingulum bundle contributed to the classification of unmedicated OCD and medicated OCD in both adult and pediatric samples. The cingulum bundle contains short and long connections between the frontal lobe, parietal lobe, and temporal lobe. In short, our machine learning findings suggest common patterns of white matter abnormalities in adult and pediatric OCD, as well as distinct patterns consistent with prior work [2].

The classification model of unmedicated OCD from HC showed greater accuracies than the model classifying all OCD from HC. This would suggest medication status likely confounds the white matter microstructure of OCD patients. In the literature, the causal effects of medication, Serotonin Reuptake Inhibitor (SSRI), on the white matter microstructure remain unclear: No randomized controlled trial exists. Nevertheless, given the key role of serotonin in neurodevelopment including gliogenesis [35], changes in extracellular serotonin levels in the brain owing to SSRI may impact the integrity of the white matter fibers. Prior correlational research supports this. A cross-sectional study shows a decrease in FA in the sagittal striatum associated with medication use in adults with OCD compared to unmedicated

OCD [15]; longitudinal clinical studies show a decrease in MD of the midbrain white matter bundles after 12-week administration of SSRI [36], a decrease in MD in the frontal regions and the corpus callosum [37]. Though some of these correlational findings might indicate causal effects of SSRI on the white matter, nevertheless, without direct causal evidence it is still unclear if the associations result from the neurobiological effects of SSRI, symptom improvement, or both. A practical implication of our finding is that the diffusion white matter-based model presents a particular utility in classifying medication naïve individuals with OCD from healthy individuals. Though not reaching the clinical utility yet (e.g., around AUC of 80%), with further research (perhaps with the integration of brain, genetic, and behavioral multi-modal data [38]), the white matter diffusion estimates might be used to predict the risk for OCD. Future research may test whether the models trained on medication naïve OCD patients—perhaps capable of learning the neurobiological patterns underlying the OCD without medication confounding—may be used for related tasks (e.g., via representational learning [39]).

There are limitations of this study. Firstly, the imaging acquisition was not harmonized across the sites, so we could not test whether the suboptimal model performance or the cross-site variability might result from the issues of the data or not. Given the sensitivity of the anisotropy and diffusivity estimates depending on the pulse sequence designs (e.g., the number of directions, b-values) [40], despite the harmonized image processing method (TBSS), the remaining data quality and validity issues perhaps may have worked against model performance. Secondly, since only the image-derived phenotypes were available from the

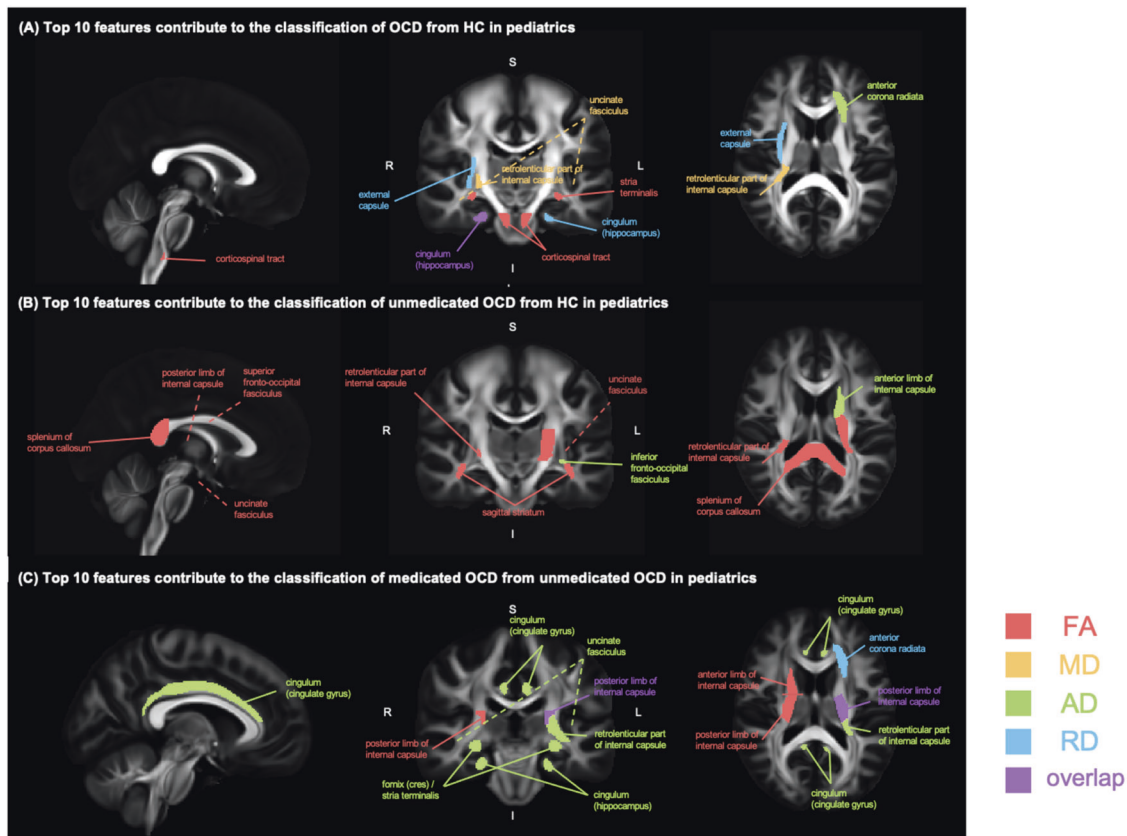


Fig. 5 Top 10 features of classification models in pediatrics. **A** Top 10 features contribute to the classification of OCD from HC in pediatrics. **B** Top 10 features contribute to the classification of unmedicated OCD from HC in pediatrics. **C** Top 10 features contribute to the classification of medicated OCD from unmedicated OCD in pediatrics. Note: The color legend represents DTI measures: red for FA, yellow for MD, green for AD, and blue for RD. Regions with multiple DTI measures are highlighted in purple.

ENIGMA consortium, but not the raw images, our results are only limited to a single type of analysis (TBSS) and metrics (diffusivity and anisotropy). Thirdly, our adult samples were larger than the pediatric samples, so our machine learning methods may have resulted in more optimized learning outcomes for adult samples.

In conclusion, using the largest multisite DTI with harmonized image processing, our investigation indicates that machine learning models currently allow only poor-to-modest classification power, but that capture meaningful multivariate patterns of white matter features relevant to the neurobiology of OCD. Accuracy is largely constrained by site variability, indicating room for future improvement.

DATA AVAILABILITY

The data that support the findings of this study are not openly available due to reasons of sensitivity and are available from the ENIGMA consortium (<https://enigma.ini.usc.edu/>) upon reasonable request.

CODE AVAILABILITY

The computer code for the above-described analyses is publicly available (<https://github.com/Transconnectome/ENIGMA-OCD>).

REFERENCES

- Fawcett EJ, Power H, Fawcett JM. Women Are at Greater Risk of OCD Than Men. *J Clin Psychiatry*. 2020;81:19r13085.
- Boedhoe PSW, Schmaal L, Abe Y, Ameis SH, Arnold PD, Batistuzzo MC, et al. Distinct Subcortical Volume Alterations in Pediatric and Adult OCD: A Worldwide Meta- and Mega-Analysis. *Am J Psychiatry*. 2017;174:60–69.
- de Wit SJ, Alonso P, Schveren L, Mataix-Cols D, Lochner C, Menchón JM, et al. Multicenter Voxel-Based Morphometry Mega-Analysis of Structural Brain Scans in Obsessive-Compulsive Disorder. *Am J Psychiatry*. 2014;171:340–9.
- Norman LJ, Carlisi C, Lukito S, Hart H, Mataix-Cols D, Radua J, et al. Structural and Functional Brain Abnormalities in Attention-Deficit/Hyperactivity Disorder and Obsessive-Compulsive Disorder. *JAMA Psychiatry*. 2016;73:815.
- Stein DJ, Costa DLC, Lochner C, Miguel EC, Reddy YCJ, Shavitt RG, et al. Obsessive-compulsive disorder. *Nat Rev Dis Prim*. 2019;5:52.
- Chamberlain SR, Menzies L, Hampshire A, Suckling J, Fineberg NA, del Campo N, et al. Orbitofrontal Dysfunction in Patients with Obsessive-Compulsive Disorder and Their Unaffected Relatives. *Science*. 2008;321:421–2.
- Menzies L, Chamberlain SR, Laird AR, Thelen SM, Sahakian BJ, Bullmore ET. Integrating evidence from neuroimaging and neuropsychological studies of obsessive-compulsive disorder: The orbitofronto-striatal model revisited. *Neurosci Biobehav Rev*. 2008;32:525–49.
- Bruin W, Denys D, van Wingen G. Diagnostic neuroimaging markers of obsessive-compulsive disorder: Initial evidence from structural and functional MRI studies. *Prog Neuro Psychopharmacol Biol Psychiatry*. 2019;91:49–59.
- Bruin W, Taylor L, Thomas RM, Shock JP, Zhutovsky P, Abe Y, et al. Structural neuroimaging biomarkers for obsessive-compulsive disorder in the ENIGMA-OCD consortium: medication matters. *Transl Psychiatry*. 2020;10:1–12.
- Zhou C, Cheng Y, Ping L, Xu J, Shen Z, Jiang L, et al. Support Vector Machine Classification of Obsessive-Compulsive Disorder Based on Whole-Brain Volumetry and Diffusion Tensor Imaging. *Front Psychiatry*. 2018;9:524.
- Yun J-Y, Jang JH, Kim SN, Jung WH, Kwon JS. Neural Correlates of Response to Pharmacotherapy in Obsessive-Compulsive Disorder: Individualized Cortical Morphology-Based Structural Covariance. *Prog Neuro Psychopharmacol Biol Psychiatry*. 2015;63:126–33.
- Hoexter MQ, Miguel EC, Diniz JB, Shavitt RG, Busatto GF, Sato JR. Predicting obsessive-compulsive disorder severity combining neuroimaging and machine learning methods. *J Affect Disord*. 2013;150:1213–6.
- Marek S, Tervo-Clemmens B, Calabro FJ, Montez DF, Kay BP, Hatoum AS, et al. Reproducible brain-wide association studies require thousands of individuals. *Nature*. 2022;603:654–60.

14. Radua J, Grau M, van den Heuvel O, Thiebaut de Schotten M, Stein D, Canales-Rodríguez E, et al. Multimodal Voxel-Based Meta-Analysis of White Matter Abnormalities in Obsessive–Compulsive Disorder. *Neuropsychopharmacology*. 2014;39:1547–57.
15. Piras F, Piras F, Abe Y, Agarwal SM, Anticevic A, Ameis S, et al. White matter microstructure and its relation to clinical features of obsessive–compulsive disorder: findings from the ENIGMA OCD Working Group. *Translational Psychiatry* 2021;11:173.
16. Goodman WK, Price LH, Rasmussen SA, Mazure C, Fleischmann RL, Hill CL, et al. The Yale-Brown Obsessive Compulsive Scale. I. Development, use, and reliability. *Arch Gen Psychiatry*. 1989;46:1006–11.
17. Scahill L, Riddle MA, McSwiggin-Hardin M, Ort SI, King RA, Goodman WK, et al. Children's Yale-Brown Obsessive Compulsive Scale: Reliability and Validity. *J Am Acad Child Adolesc Psychiatry*. 1997;36:844–52.
18. van der Laan MJ, Polley EC, Hubbard AE. Super Learner. *Stat Appl Genet Mol Biol*. 2007;6:e4189.
19. Whitley D. A genetic algorithm tutorial. *Stat Comput*. 1994;4:9016.
20. Robin X, Turck N, Hainard A, Tiberti N, Lisacek F, Sanchez J-C, et al. pROC: an open-source package for R and S+ to analyze and compare ROC curves. *BMC Bioinforma*. 2011;12:77.
21. Fortin J-P, Parker D, Tunç B, Watanabe T, Elliott MA, Ruparel K, et al. Harmonization of multi-site diffusion tensor imaging data. *NeuroImage*. 2017;161:149–70.
22. Fortin J-P, Cullen N, Sheline YI, Taylor WD, Aselcioglu I, Cook PA, et al. Harmonization of cortical thickness measurements across scanners and sites. *NeuroImage*. 2018;167:104–20.
23. Ribeiro MT, Singh S, Guestrin C. Why Should I Trust You? In: Proceedings of the 22nd ACM SIGKDD International Conference on Knowledge Discovery and Data Mining - KDD '16. 2016. <https://doi.org/10.1145/2939672.2939778>.
24. Ganesh A, Ospel JM, Menon BK, Demchuk AM, McTaggart RA, Nogueira RG, et al. Assessment of Discrepancies Between Follow-up Infarct Volume and 90-Day Outcomes Among Patients With Ischemic Stroke Who Received Endovascular Therapy. *JAMA Netw Open*. 2021;4:e2132376.
25. Calhoun VD, Sui J. Multimodal Fusion of Brain Imaging Data: A Key to Finding the Missing Link(s) in Complex Mental Illness. *Biol Psychiatry Cogn Neurosci Neuroimaging*. 2016;1:230–44.
26. Kuo C-Y, Tai T-M, Lee P-L, Tseng C-W, Chen C-Y, Chen L-K, et al. Improving Individual Brain Age Prediction Using an Ensemble Deep Learning Framework. *Front Psychiatry*. 2021;12:626677.
27. Guggenmos M, Schmack K, Veer IM, Lett T, Sekutowicz M, Sebold M, et al. A multimodal neuroimaging classifier for alcohol dependence. *Sci Rep*. 2020;10:298.
28. Menon SS, Krishnamurthy K. Multimodal Ensemble Deep Learning to Predict Disruptive Behavior Disorders in Children. *Front Neuroinformatics*. 2021;15:742807.
29. Guo C, Ferreira D, Fink K, Westman E, Granberg T. Repeatability and reproducibility of FreeSurfer, FSL-SIENAX and SPM brain volumetric measurements and the effect of lesion filling in multiple sclerosis. *Eur Radiol*. 2019;29:1355–64.
30. Liu L, Liu J, Yang L, Wen B, Zhang X, Cheng J, et al. Accelerated Brain Aging in Patients With Obsessive-Compulsive Disorder. *Front Psychiatry*. 2022;13:852479.
31. Han LKM, Schnack HG, Brouwer RM, Veltman DJ, van der Wee NJA, van Tol M-J, et al. Contributing factors to advanced brain aging in depression and anxiety disorders. *Transl Psychiatry*. 2021;11:1–11.
32. Koch K, Reeb TJ, Rus OG, Zimmer C, Zaudig M. Diffusion tensor imaging (DTI) studies in patients with obsessive-compulsive disorder (OCD): A review. *J Psychiatr Res*. 2014;54:26–35.
33. Simpson HB, van den Heuvel OA, Miguel EC, Reddy YCJ, Stein DJ, Lewis-Fernández R, et al. Toward identifying reproducible brain signatures of obsessive-compulsive profiles: rationale and methods for a new global initiative. *BMC Psychiatry*. 2020;20:68.
34. Spalletta G, Piras F, Fagioli S, Caltagirone C, Piras F. Brain microstructural changes and cognitive correlates in patients with pure obsessive compulsive disorder. *Brain Behav*. 2014;4:261–77.
35. Millard SJ, Weston-Green K, Newell KA. The effects of maternal antidepressant use on offspring behaviour and brain development: Implications for risk of neurodevelopmental disorders. *Neurosci Biobehav Rev*. 2017;80:743–65.
36. Fan Q, Yan X, Wang J, Chen Y, Wang X, Li C, et al. Abnormalities of White Matter Microstructure in Unmedicated Obsessive-Compulsive Disorder and Changes after Medication. *PLoS ONE*. 2012;7:e35889.
37. Seiger R, Gryglewski G, Klöbl M, Kautzky A, Godbersen GM, Rischka L, et al. The Influence of Acute SSRI Administration on White Matter Microstructure in Patients Suffering From Major Depressive Disorder and Healthy Controls. *Int J Neuropsychopharmacol*. 2021;24:542–50.
38. Rahaman MA, Chen J, Fu Z, Lewis N, Iraj A, Calhoun VD. Multi-modal deep learning of functional and structural neuroimaging and genomic data to predict mental illness. *IEEE Xplore*. 2021:3267-72. <https://ieeexplore.ieee.org/abstract/document/9630693>. Accessed 25 July 2022.
39. Arol A, Fu Z, Salman M, Silva R, Du Y, Plis S, et al. Deep learning encodes robust discriminative neuroimaging representations to outperform standard machine learning. *Nat Commun*. 2021;12:353.
40. Ni H, Kavcic V, Zhu T, Ekholm S, Zhong J. Effects of number of diffusion gradient directions on derived diffusion tensor imaging indices in human brain. *AJNR Am J Neuroradiol*. 2006;27:1776–81.

ACKNOWLEDGEMENTS

This work was supported by the National Research Foundation of Korea(NRF) grant funded by the Korean government(MSIT) (No. 2019H1D3A2A01102270, 2021R1C1C1006503, 2021K1A3A1A2103751212, 2021M3E5D2A01022515, RS-2023-00266787, RS-2023-00265406), Creative-Pioneering Researchers Program through Seoul National University (No. 200-20230058), Semi-Supervised Learning Research Grant by SAMSUNG (No.A0426-20220118), Institute of Information & communications Technology Planning & Evaluation (IITP) grant funded by the Korea government(M-SIT) [NO.2021-0-01343, Artificial Intelligence Graduate School Program (Seoul National University)], and the H2O.ai Academic Program at H2O Inc., CA, USA to JC; by Grant No. K01MH122774 and Brain and Behavior Research Foundation Grant 07040 to XZ, Grant No. R01MH116147, P41EB015922 to PMT, funding of Michael Smith Health Research BC to Dr. FJ-F, IOCDF Innovator Award 2021 to CV, AMED Brain/MINDS Beyond Program Grant No. JP22dm0307002, JSPS KAKENHI Grants No. 22H01090, 19K03309 to YH (PI), FAPESP 18/21934-5 and 21/05331-8 to JRS, PI19/01171, 2017 SGR 1247 to CS-M, JP22dm0307008 to YS; SR/50/HS/0016/2011, BT/PR13334/Med/30/259/2009 to YCJR, DST INSPIRE faculty grant IFA12-LSBM-26, BT/06/IYBA/2012 to JCN by the India government; the Wellcome-DBT India Alliance grant to GV (500236/Z/11/Z); Marató TV3 Foundation Grant 091510 and Carlos III Health Institute PI11/01419 to RC; K24MH121571 from U.S. National Institute of Mental Health to CPittenger; the Japan Society for the Promotion of Science (KAKENHI Grant No. 18K15523) to YA; European Union projects TACTICS (grant 278948) and CANDY (grant 847818) to JKB; Río Hortega grant (CM21/00278) to SBertolin; Sao Paulo Research Foundation (FAPESP grants #2018/21934-5 and #2021/05332-8); the Wellcome Trust-DBT India Alliance Early Career Fellowship grant (IA/CPHE/18/1/503956) to VS; National Research Foundation of South Africa (Grants No. 78829) to CL; Scientific productivity grant from National Council for Scientific and Technological Development (CNP)#307386/2021-0 to RGS; the British Columbia Children's Hospital to SES.

AUTHOR CONTRIBUTIONS

Data collection: YA, PA, SA, AA, PDA, SBalachander, NBanaj, NBargallo, MCB, FB, Sara Bertolin, J-CB, IB, SBrem, BPB, JKB, RC, YC, RBC, AC, BC, SD, BAE, SF, MF, J-PF, RG, PG, KH, BH, YH, MQH, MH, HH, CH, TI, NJ, AJ, FJ-F, SK, NK, CK, MK, KK, GK, JSK, LL, JLee, CL, JLu, DRM, IM-Z, YM, KM, MPM, JMM, LM, PSM, PM, JCN, JN, NS, AEO, JO, JCP, CPriello, MP-P, CPittenger, SP, ER, YCJR, DvR, YS, JRS, CS, RGS, ZS, ES, VS, CS-M, NS, MMS, GS, ERS, SES, PRS, SIT, DV, GV, CV, SW, ZW, AW, LW, JX, KY, J-YY, MZ, QZ, XZ, PMT, WBB, GAVW, FedericaP, FabrizioP, DJS, OAvdH, HBS, RM.

FUNDING

Open Access funding enabled and organized by Seoul National University.

COMPETING INTERESTS

The authors declare no competing interests.

ADDITIONAL INFORMATION

Supplementary information The online version contains supplementary material available at <https://doi.org/10.1038/s41380-023-02392-6>.

Correspondence and requests for materials should be addressed to Jiook Cha.

Reprints and permission information is available at <http://www.nature.com/reprints>

Publisher's note Springer Nature remains neutral with regard to jurisdictional claims in published maps and institutional affiliations.



Open Access This article is licensed under a Creative Commons Attribution 4.0 International License, which permits use, sharing, adaptation, distribution and reproduction in any medium or format, as long as you give appropriate credit to the original author(s) and the source, provide a link to the Creative Commons licence, and indicate if changes were made. The images or other third party material in this article are included in the article's Creative Commons licence, unless indicated otherwise in a credit line to the material. If material is not included in the

article's Creative Commons licence and your intended use is not permitted by statutory regulation or exceeds the permitted use, you will need to obtain permission directly from the copyright holder. To view a copy of this licence, visit <http://creativecommons.org/licenses/by/4.0/>.

© The Author(s) 2024, corrected publication 2024

¹Department of Psychology, College of Social Sciences, Seoul National University, Seoul, Republic of Korea. ²Department of Brain and Cognitive Sciences, College of Natural Sciences, Seoul National University, Seoul, Republic of Korea. ³Graduate School of Medical Science, Kyoto Prefectural University of Medicine, Department of Psychiatry, Kyoto City, Japan. ⁴Bellvitge Biomedical Research Institute-IDIBELL, Bellvitge University Hospital, Barcelona, Spain. ⁵CIBER of Mental Health (CIBERSAM), Carlos III Health Institute, Madrid, Spain. ⁶Department of Clinical Sciences, University of Barcelona, Barcelona, Spain. ⁷The Margaret and Wallace McCain Centre for Child, Youth & Family Mental Health and Campbell Family Mental Health Research Institute, Centre for Addiction and Mental Health, Toronto, ON, Canada. ⁸Department of Psychiatry, University of Toronto, Toronto, ON, Canada. ⁹Program in Neurosciences and Mental Health, The Hospital for Sick Children, Toronto, ON, Canada. ¹⁰Department of Psychiatry, Yale University School of Medicine, New Haven, CT 06510, USA. ¹¹The Mathison Centre for Mental Health Research & Education, Hotchkiss Brain Institute, Cumming School of Medicine, University of Calgary, Calgary, AB, Canada. ¹²Departments of Psychiatry and Medical Genetics, Cumming School of Medicine, University of Calgary, Calgary, AB, Canada. ¹³ OCD clinic, Department of Psychiatry, National Institute of Mental Health And Neurosciences (NIMHANS), Bangalore, India. ¹⁴Laboratory of Neuropsychiatry, Department of Clinical and Neuroscience and Neurorehabilitation, IRCCS Santa Lucia Foundation, Rome, Italy. ¹⁵Center of Image Diagnostic, Hospital Clínic de Barcelona, Barcelona, Spain. ¹⁶Magnetic Resonance Image Core Facility, Institut d'Investigacions Biomèdiques August Pi i Sunyer (IDIBAPS), Barcelona, Spain. ¹⁷Departamento e Instituto de Psiquiatria do Hospital das Clinicas, IPQ HCFMUSP, Faculdade de Medicina, Universidade de Sao Paulo, Sao Paulo, SP, Brazil. ¹⁸Department of Methods and Techniques in Psychology, Pontifical Catholic University, São Paulo, SP, Brazil. ¹⁹Vita-Salute San Raffaele University, Milano, Italy. ²⁰Psychiatry & Clinical Psychobiology, Division of Neuroscience, IRCCS Scientific Institute Ospedale San Raffaele, Milano, Italy. ²¹Bellvitge Biomedical Research Institute-IDIBELL, Bellvitge University Hospital, Barcelona, Spain. ²²Department of Psychology, Humboldt-Universität zu Berlin, Berlin, Germany. ²³Department of Clinical Neuroscience, Centre for Psychiatric Research and Education, Karolinska Institutet, Stockholm, Sweden. ²⁴Department of Medical Psychology, Medical School Hamburg, Hamburg, Germany. ²⁵Department of Child and Adolescent Psychiatry and Psychotherapy, University Hospital of Psychiatry Zurich, University of Zurich, Zurich, Switzerland. ²⁶Neuroscience Center Zurich, University of Zurich and ETH Zurich, Zurich, Switzerland. ²⁷McLean Hospital, Belmont, MA, USA. ²⁸Department of Psychiatry, Harvard Medical School, Boston, MA, USA. ²⁹Radboudumc, Department of Cognitive Neuroscience, Nijmegen, The Netherlands. ³⁰Karakter Child and Adolescent Psychiatry University Center, Nijmegen, The Netherlands. ³¹Department of Child and Adolescent Psychiatry and Psychology, Institute of Neurosciences, Hospital Clínic Universitari, Barcelona, Spain. ³²Institut d'Investigacions Biomèdiques August Pi i Sunyer (IDIBAPS), Barcelona, Spain. ³³Department of Medicine, University of Barcelona, Barcelona, Spain. ³⁴Coimbra Institute for Biomedical Imaging and Translational Research (CIBIT), University of Coimbra, 3000-548 Coimbra, Portugal. ³⁵Institute for Nuclear Sciences Applied to Health (ICNAS), University of Coimbra, 3000-548 Coimbra, Portugal. ³⁶Faculty of Medicine, University of Coimbra, 3000-548 Coimbra, Portugal. ³⁷Department of Psychiatry, First Affiliated Hospital of Kunming Medical University, Kunming, China. ³⁸Research Center for Child Mental Development, Chiba University, Chiba, Japan. ³⁹United Graduate School of Child Development, Osaka University, Kanazawa University, Hamamatsu University, Chiba University and University of Fukui, Suita, Japan. ⁴⁰Life and Health Sciences Research Institute (ICVS), School of Medicine, University of Minho, Braga, Portugal. ⁴¹ICVS/3B's, PT Government Associate Laboratory, Braga/Guimaraes, Portugal. ⁴²Clinical Academic Center - Braga, Braga, Portugal. ⁴³Psychiatry & Clinical Psychobiology Unit, Division of Neuroscience, Scientific Institute Ospedale San Raffaele, Milano, Italy. ⁴⁴Department of Psychiatry and Behavioral Sciences, Albert Einstein College of Medicine, Bronx, NY, USA. ⁴⁵Columbia University Medical College, Columbia University, New York, NY, USA. ⁴⁶SAMRC Genomics of Brain Disorders Unit, Department of Psychiatry, Cape Town, South Africa. ⁴⁷Hospital of Molde, Møre og Romsdal Hospital Trust, Molde, Norway. ⁴⁸Bergen Center for Brain Plasticity, Haukeland University Hospital, Bergen, Norway. ⁴⁹Centre for Crisis Psychology, University of Bergen, Bergen, Norway. ⁵⁰Department of Psychiatry, University of Michigan Medical School, Ann Arbor, MI, USA. ⁵¹Highfield Unit Oxford, Warneford Hospital, Warneford Lane, Headington, Oxford, Oxfordshire OX3 7JX, UK. ⁵²Shanghai Mental Health Center, Shanghai, China. ⁵³Level, academic center for child and adolescent care, Amsterdam, The Netherlands. ⁵⁴Department of Child and Adolescent Psychiatry, Amsterdam UMC, Amsterdam, The Netherlands. ⁵⁵Department of Communication Sciences and Disorders, University of Mississippi, Oxford, MS, USA. ⁵⁶Imaging Genetics Center, Mark and Mary Stevens Neuroimaging and Informatics Institute, Keck School of Medicine, University of Southern California, Marina del Rey, Los Angeles, CA, USA. ⁵⁷Department of Psychiatry University of Oxford, Warneford Hospital, Oxford OX3 7JX, UK. ⁵⁸Department of Psychiatry, University of British Columbia, Vancouver, BC, Canada. ⁵⁹BC Children's Hospital Research Institute, Vancouver, BC, Canada. ⁶⁰Amsterdam UMC, Vrije Universiteit Amsterdam, Department of Psychiatry, Amsterdam Neuroscience, Amsterdam, The Netherlands. ⁶¹Amsterdam UMC, Vrije Universiteit Amsterdam, Department of Anatomy and Neurosciences, Amsterdam Neuroscience, Amsterdam, The Netherlands. ⁶²Department of Neuropsychiatry, Seoul National University Hospital, Seoul, Republic of Korea. ⁶³Department of Psychiatry, Seoul National University College of Medicine, Seoul, Republic of Korea. ⁶⁴TUM-Neuroimaging Center (TUM-NIC) of Klinikum rechts der Isar, Technische Universität München, München, Germany. ⁶⁵Department of Diagnostic and Interventional Neuroradiology, School of Medicine, Technical University of Munich, Munich, Germany. ⁶⁶Department of Clinical Psychology, University of Bergen, Bergen, Norway. ⁶⁷Department of Brain and Cognitive Sciences, Seoul National University College of Natural Sciences, Seoul, Republic of Korea. ⁶⁸Institute of Human Behavioral Medicine, SNU-MRC, Seoul, Republic of Korea. ⁶⁹Department of Psychiatry, Uijeongbu Eulji Medical Center, Uijeongbu, Republic of Korea. ⁷⁰SAMRC Unit on Risk & Resilience in Mental Disorders, Department of Psychiatry, Stellenbosch University, Stellenbosch, South Africa. ⁷¹Department of Psychiatry, First Affiliated Hospital of Kunming Medical University, Kunming, China. ⁷²Graduate School of Systemic Neurosciences, Ludwig-Maximilians-University, Munich, Germany. ⁷³Department of Radiology, Bellvitge University Hospital, Barcelona, Spain. ⁷⁴Chiba University Hospital, Chiba University, Chiba, Japan. ⁷⁵LIM 23, Instituto de Psiquiatria, Hospital das Clinicas da Faculdade de Medicina da Universidade de Sao Paulo, Sao Paulo, Brazil. ⁷⁶Faculty of Medicine, City University of Sao Paulo, Sao Paulo, Brazil. ⁷⁷Anxiety Treatment and Research Clinic, St. Joseph's Hamilton Healthcare, Hamilton, ON, Canada. ⁷⁸Departments of Psychiatry and Behavioural Neurosciences, McMaster University, Hamilton, ON, Canada. ⁷⁹Psychological Neuroscience Lab, CIPsi, School of Psychology, University of Minho, Braga, Portugal. ⁸⁰Department of Psychiatry, Graduate School of Medical Science, Kyoto Prefectural University of Medicine, Kyoto, Japan. ⁸¹University of Illinois at Urbana-Champaign, Champaign, IL, USA. ⁸²Departamento de Psicología Básica, Clínica y Psicobiología, Universitat Jaume I, Castelló de la Plana, Spain. ⁸³Department of Psychology, Yale University, New Haven, CT, USA. ⁸⁴Child Study Center, Yale University, New Haven, CT, USA. ⁸⁵Center for Brain and Mind Health, Yale University, New Haven, CT, USA. ⁸⁶Radboud University Medical Center, Donders Institute for Brain, Cognition and Behavior, Department of Cognitive Neuroscience, Nijmegen, The Netherlands. ⁸⁷ATR Brain Information Communication Research Laboratory Group, Kyoto, Japan. ⁸⁸Center of Mathematics, Computing and Cognition, Universidade Federal do ABC, Santo André, Brazil. ⁸⁹Big Data, Hospital Israelita Albert Einstein, São Paulo, Brazil. ⁹⁰Departamento de Psiquiatria, Hospital das Clinicas HCFMUSP, Faculdade de Medicina, Universidade de Sao Paulo, Sao Paulo, SP, Brazil. ⁹¹Department of Cognitive Behavioral Physiology, Graduate School of Medicine, Chiba University, Chiba, Japan. ⁹²National Institute of Mental Health and Neurosciences, Department of Integrative Medicine, Bengaluru, India. ⁹³Department of Psychiatry and Behavioural Neurosciences, McMaster University, Hamilton, Ontario, Canada. ⁹⁴Offord Centre for Child Studies, Hamilton, Ontario, Canada. ⁹⁵Department of Social Psychology and Quantitative Psychology, University of Barcelona, Barcelona, Spain. ⁹⁶Division of Neuropsychiatry, Menninger Department of Psychiatry and Behavioral Science, Baylor College of Medicine, Houston, TX, USA. ⁹⁷Department of Psychiatry, New York University School of Medicine, New York, NY, USA. ⁹⁸Clinical Research, Nathan Kline Institute for Psychiatric Research, Orangeburg, NY, USA. ⁹⁹British Columbia Children's Hospital, Psychiatry, Vancouver, BC, Canada. ¹⁰⁰British Columbia Mental Health and Substance Use Services Research Institute, Vancouver, BC, Canada. ¹⁰¹Departments of Psychiatry and Neuroscience, Icahn School of Medicine at Mount Sinai, New York, NY, USA. ¹⁰²Mental Illness Research, Education and Clinical Center, James J. Peters VA Medical Center, Bronx, NY, USA. ¹⁰³Weill-Cornell Medicine Qatar, Education City, Doha, Qatar. ¹⁰⁴Amsterdam Neuroscience, Compulsivity, Impulsivity & Attention program, Amsterdam, The Netherlands. ¹⁰⁵Shanghai Mental Health Center, Shanghai Jiao Tong University School of Medicine, Shanghai, China. ¹⁰⁶Norwegian University of Science and Technology (NTNU), Faculty of Medicine, Regional Centre for Child and Youth Mental Health and Child Welfare (RKBU Central Norway), Klostergata 46, 7030 Trondheim, Norway. ¹⁰⁷Department of Internal Medicine, First Affiliated Hospital of Kunming Medical University, Kunming, China. ¹⁰⁸Department of Radiology, Graduate School of Medical Science, Kyoto Prefectural University of Medicine, Kyoto, Japan. ¹⁰⁹Seoul National University Hospital, Seoul, Republic of Korea. ¹¹⁰Yeongeon Student Support Center, Seoul National University College of Medicine,

Seoul, Republic of Korea. ¹¹¹Institute of Medical Science and Technology, Shahid Beheshti University, Tehran, Iran. ¹¹²Department of Psychiatry, Columbia University Irving Medical Center, New York, NY, USA. ¹¹³New York State Psychiatric Institute, New York, NY, USA. ¹¹⁴Amsterdam UMC, Universiteit van Amsterdam, Department of Psychiatry, Amsterdam, The Netherlands. ¹¹⁵Department of Psychiatry and Mental Health, University of Cape Town, Cape Town, South Africa. ¹¹⁶SAMRC Unit on Risk & Resilience in Mental Disorders, Cape Town, South Africa. ¹⁴⁸These authors contributed equally: Bo-Gyeom Kim, Gakyung Kim. *A list of authors and their affiliations appears at the end of the paper. [✉]email: connectome@snu.ac.kr

ENIGMA-OCD WORKING GROUP

Yoshinari Abe ³, Pino Alonso ^{4,5,6}, Stephanie Ameis ^{7,8,9}, Alan Anticevic¹⁰, Honami Arai³⁸, Ana Isabel Araújo^{34,35}, Kentaro Araki³⁸, Paul D. Arnold^{11,27}, Justin T. Baker^{13,28}, Srinivas Balachander¹³, Nerisa Banaj ¹⁴, Núria Bargalló^{15,16,17}, Marcelo C. Batistuzzo ^{17,18}, Francesco Benedetti ^{19,20}, Sara Bertolin^{21,117}, John R. Best^{58,118}, Jan Carl Beucke^{22,23,24}, Premika S. W. Boedhoe¹¹⁹, Irene Bollettini ²⁰, Sven Bölte¹²⁰, Vilde Brecke⁴⁸, Silvia Brem^{25,26}, Brian P. Brennan ^{27,28}, Willem B. Bruin^{104,114}, Jan K. Buitelaar^{30,31}, Rosa Calvo^{31,32,33,117}, Carolina Cappi⁹⁰, Joao Castelhamo^{34,35}, Miguel Castelo-Branco^{34,35,36}, Wei Chen¹²¹, Yuqi Cheng³⁷, Ritu Bhusal Chhatkuli^{38,39}, Sutoh Chihiro¹²², Kang Ik Kevin Cho^{2,123}, Sunah Choi², Valentina Ciullo¹⁴, Ana Coelho^{40,41,42}, Daniel Costa⁹⁰, Beatriz Couto^{40,41,42}, Nan Dai³⁷, Sara Dallspezia⁴³, Shareefa Dalvie¹²⁴, Damiaan Denys¹²⁵, Juliana B. Diniz⁹⁰, Isabel C. Duarte^{34,35}, Benjamin A. Ely ⁴⁴, Calesella Federico¹⁹, Sónia Ferreira^{40,41,42}, Jamie D. Feusner¹²⁶, Kate D. Fitzgerald⁵⁰, Martine Fontaine⁴⁵, Jean-Paul Fouché⁴⁶, Egill Axfjord Fridgeirsson¹²⁵, Rachael Grazioplene ¹⁰, Edna Grünblatt^{25,26}, Patricia Gruner¹⁰, Kristen Hagen^{47,48}, Sayo Hamatani^{38,39}, Gregory Hanna⁵⁰, Bjarne Hansen^{48,49}, Mengxin He³⁷, Odile A. van den Heuvel^{60,61,104}, Yoshiyuki Hirano ^{38,39}, Marcelo Q. Höxter^{17,90}, Morgan Hough⁹⁰, Hao Hu⁵², Chaim Huyser ^{53,54}, Keisuke Ikari¹²⁷, Toshikazu Ikuta ⁵⁵, Jonathan Ipser¹²⁸, Neda Jahanshad⁵⁶, Anthony James ⁵⁷, Fern Jaspers-Fayer ^{58,59}, Hongyan Jiang³⁷, Linling Jiang³⁷, Niels T. de Joode¹¹⁹, Selina Kasprzak^{60,61}, Norbert Kathmann²⁶, Christian Kaufmann²², Minah Kim ^{62,63}, Taekwan Kim^{2,129}, Hitomi Kitagawa³⁸, Kathrin Koch ^{64,65}, Masaru Kuno^{38,39}, Gerd Kvale^{48,66}, Yoo Bin Kwak², Jun Soo Kwon^{2,63,68}, Luisa Lazaro ^{5,31,32,33}, Junhee Lee ^{62,69}, Wieke van Leeuwen¹²⁵, Chiang-shan Ray Li¹⁰, Na Li³⁹, Yanni Liu⁵⁰, Fang Iiu³⁷, Christine Lochner ⁷⁰, Antonio Carlos Lopes⁹⁰, Jin Lu³⁷, Yuri Milaneschi¹³⁰, Daniela Rodriguez Manrique^{64,65,72}, Hein van Marle¹³¹, Rachel Marsh ⁴⁵, Ignacio Martinez-Zalacain ^{4,73}, Sergi Mas^{132,133,134}, Yoshitada Masuda⁷⁴, David Mataix-Cols²³, Maria Alice de Mathis^{75,76}, Koji Matsumoto⁷⁴, Maria Paula Mazieiro^{75,76}, Sarah Medland¹³⁵, Renata Melo⁹⁰, Jose M. Menchón ^{4,5,6}, Euripedes C. Miguel⁹⁰, Luciano Minuzzi^{77,78}, Pedro Silva Moreira ^{40,41,79}, Astrid Morer^{33,133,136}, Pedro Morgado^{40,41,42}, Alessandro S. De Nadai¹³⁷, Tomohiro Nakao¹²⁷, Janardhanan C. Narayanaswamy¹³, Jin Narumoto⁸⁰, Masato Nihei³⁸, Luke Norman¹³⁸, Erika L. Nurmi¹³⁹, Joseph O'Neil¹⁴⁰, Sanghoon Oh^{63,69}, Sho Okawa¹²², Ana E. Ortiz^{31,32,33}, Junko Ota^{38,39}, Jose C. Pariente ¹⁶, Chris Perriello⁸¹, John C. Piacentini¹⁴⁰, Maria Picó-Pérez^{40,41}, Federica Piras¹⁴, Fabrizio Piras ¹⁴, Christopher Pittenger ^{10,83,84,85}, Sara Poletti ²⁰, Eva Real^{5,6}, Y.C. Janardhan Reddy¹³, Natalia Rodriguez¹³², Daan van Rooij⁸⁶, Yuki Sakai ^{80,87}, João R. Sato^{88,89}, Cinto Segalas^{2,6}, Roseli G. Shavitt⁹⁰, Zonglin Shen³⁷, Eiji Shimizu ^{38,39,91}, Venkataram Shivakumar⁹², Noam Soreni^{93,94}, Renata Silva¹⁷, Helen Blair Simpson⁴⁵, Noam Soreni^{141,142}, Carles Soriano-Mas ^{5,6,95}, Nuno Sousa ^{40,41,42}, Mafalda Machado Sousa^{40,41,42}, Gianfranco Spalletta^{14,96}, Dan J. Stein ^{115,116}, Emily R. Stern^{97,98}, Michael Stevens^{143,144}, S. Evelyn Stewart ^{58,99,100}, Anouk van der Straten¹²⁵, Philip R. Szeszko^{101,102}, Jumpei Takahashi³⁸, Tais Tanamatis⁹⁰, Jinsong Tang¹⁴⁵, Rajat Thomas¹⁰³, Sophia I. Thomopoulos⁵⁶, Paul M. Thompson⁵⁶, Anders Lillevik Thorsen^{48,49}, David Tolin^{143,144}, Anne Uhlmann¹⁴⁶, Benedetta Vai²⁰, Ysbrand D. van der Werf⁶¹, Daniela Vecchio¹⁴, Dick J. Veltman¹¹⁹, Ganesan Venkatasubramanian¹³, Nora Vetter^{133,147}, Chris Vriend^{60,61,103}, Susanne Walitza^{25,26}, Zhen Wang ¹⁰⁵, Jicai Wang³⁷, Anri Watanabe ⁸⁰, Cees J. Weeland¹¹⁹, Guido A. van Wingen^{104,114}, Stella J. de Wit¹¹⁹, Nicole Wolff¹³³, Lidewij Wolters¹⁰⁶, Jian Xu¹⁰⁷, Xiufeng Xu³⁷, Kei Yamada¹⁰⁸, Tokiko Yoshida^{38,39}, Je-Yeon Yun ^{109,110}, Mojtaba Zarei¹¹¹ and Fengrui Zhang¹²¹, Qing Zhao¹⁰⁵ and Xi Zhu^{112,113}

¹¹⁷CIBERSAM, Barcelona, Spain. ¹¹⁸Gerontology Research Centre, Simon Fraser University, Burnaby, BC, Canada. ¹¹⁹Amsterdam UMC, Vrije Universiteit Amsterdam, Department of Psychiatry, Department of Anatomy & Neurosciences, Amsterdam, The Netherlands. ¹²⁰Department of Women's & Children's Health, Center for Psychiatry Research, Karolinska Institutet, Stockholm, Sweden. ¹²¹Magnetic Resonance Image Center, First Affiliated Hospital of Kunming Medical University, Kunming, China. ¹²²Department of Cognitive Behavioral Physiology, Graduate School of Medicine and School of Medicine, Chiba University, Chiba, Japan. ¹²³Psychiatry Neuroimaging Laboratory, Department of Psychiatry, Brigham and Women's Hospital, Harvard Medical School, Boston, MA, USA. ¹²⁴SA MRC Unit on Risk & Resilience in Mental Disorders, Department of Psychiatry and Mental Health, University of Cape Town, Cape Town, South Africa. ¹²⁵Amsterdam UMC, University of Amsterdam, Department of Psychiatry, Amsterdam Neuroscience, Amsterdam, The Netherlands. ¹²⁶Division of Neurosciences & Clinical Translation, Temerty Faculty of Medicine, University of Toronto, Toronto, ON, Canada. ¹²⁷Department of Neuropsychiatry, Graduate School of Medical Sciences, Kyushu University, Fukuoka, Japan. ¹²⁸Department of Psychiatry and Mental Health and Neuroscience Institute, Brain Behaviour Unit, University of Cape Town, Cape Town, South Africa. ¹²⁹Department of Bio and Brain Engineering, Korea Advanced Institute of Science and Technology, Daejeon, Republic of Korea. ¹³⁰Amsterdam UMC, Vrije Universiteit Amsterdam, Department of Psychiatry, Amsterdam Neuroscience, Amsterdam, The Netherlands. ¹³¹Amsterdam UMC, Vrije Universiteit, Department of Psychiatry, Amsterdam Neuroscience, Amsterdam, The Netherlands. ¹³²Department of Basic Clinical Practice, Pharmacology Unit, University of Barcelona, Barcelona, Spain. ¹³³IDIBAPS, Barcelona, Spain. ¹³⁴Centro de Investigación Biomédica en Red de salud mental (CIBERSAM), Barcelona, Spain. ¹³⁵QIMR Berghofer Medical Research Institute, Brisbane, QLD, Australia. ¹³⁶Department of Child and Adolescent Psychiatry and Psychology, Hospital Clinic of Barcelona. CIBERSAM, Barcelona, Spain. ¹³⁷Texas State University, Austin, TX, USA. ¹³⁸The National Institutes of Health (NIH), Bethesda, MD, USA. ¹³⁹Department of Psychiatry, University of California, Los Angeles, CA, USA. ¹⁴⁰Division of Child and Adolescent Psychiatry, Jane & Terry Semel Institute For Neurosciences, University of California, Los Angeles, CA, USA. ¹⁴¹Pediatric OCD Consultation Clinic, McMaster University, Hamilton, ON, Canada. ¹⁴²Anxiety Treatment and Research Center, McMaster University, Hamilton, ON, Canada. ¹⁴³Institute of Living, Hartford, CT, USA. ¹⁴⁴Yale University School of Medicine, New Haven, CT, USA. ¹⁴⁵Department of Psychiatry, Zhejiang University School of Medicine, Hangzhou, China. ¹⁴⁶Department of Child and Adolescent Psychiatry and Psychotherapy, TU Dresden, Dresden, Germany. ¹⁴⁷Department of Psychology, MSB Medical School Berlin, Berlin, Germany. A list of members and their affiliations appears in the Supplementary Information.